The Astrophysical Journal, 766:30 (9pp), 2013 March 20 doi:10.1088/0004-637X/766/1/30

THE ULTRA-LONG GAMMA-RAY BURST 111209A: THE COLLAPSE OF A BLUE SUPERGIANT?

B. Gendre[1,2,11], G. Stratta[3], J. L. Atteia[4,5], S. Basa[6], M. Boër[7,8], D. M. Coward[9], S. Cutini[1], V. D'Elia[1], E. J Howell[9], A. Klotz[4,5,8], and L. Piro[10]
[1] ASI Science Data Center, via Galileo Galilei, I-00044 Frascati, Italy
[2] Osservatorio Astronomico di Roma, OAR-INAF, Italy; bruce.gendre@gmail.com
[3] Osservatorio Astronomico di Roma, OAR-INAF, via Frascati 33, I-00040, Monte Porzio Catone, Italy
[4] Université de Toulouse, UPS-OMP, IRAP, Toulouse, France
[5] CNRS, IRAP, 14, avenue Edouard Belin, F-31400 Toulouse, France
[6] Aix Marseille Université, CNRS, LAM (Laboratoire d'Astrophysique de Marseille) UMR 7326, F-13388, Marseille, France
[7] CNRS, ARTEMIS, UMR 7250, Boulevard de l'Observatoire, BP 4229, F-06304 Nice Cedex 4, France
[8] CNRS, Observatoire de Haute-Provence, F-04870 Saint Michel l'Observatoire, France
[9] University of Western Australia, School of Physics, University of Western Australia, Crawley WA 6009, Australia
[10] Istituto di Astrofisica e Planetologia Spaziali di Roma, INAF, via fosso del cavaliere 100, I-00133 Roma, Italy
Received 2012 October 24; accepted 2013 February 8; published 2013 March 5

ABSTRACT

We present optical, X-ray and gamma-ray observations of GRB 111209A, observed at a redshift of $z = 0.677$. We show that this event was active in its prompt phase for about 25000 s, making it the longest burst ever observed. This rare event could have been detected up to $z \sim 1.4$ in gamma-rays. Compared to other long gamma-ray bursts (GRBs), GRB 111209A is a clear outlier in the energy-fluence and duration plane. The high-energy prompt emission shows no sign of a strong blackbody component, the signature of a tidal disruption event, or a supernova shock breakout. Given the extreme longevity of this event, and lack of any significant observed supernova signature, we propose that GRB 111209A resulted from the core-collapse of a low-metallicity blue supergiant star. This scenario is favored because of the necessity to supply enough mass to the central engine over a duration of thousands of seconds. Hence, we suggest that GRB 111209A could have more in common with population III stellar explosions, rather than those associated with normal long GRBs.

Key word: gamma-ray burst: individual (GRB111209A)

Online-only material: color figures

1. INTRODUCTION

Gamma-ray bursts (GRBs) are detected as brief flashes of high-energy photons typically lasting some tens of seconds (Klebesadel et al. 1973). First discovered in the 1960s, these cosmological sources are the most energetic explosions in the universe since the big bang (see Meszaros 2006 for a review). There are two main classes of GRBs with well separated properties and behaviors: long and short GRBs (Kouveliotou et al. 1993). Because of their extreme distances and diverse emission characteristics, it has been difficult to isolate a single progenitor responsible for all long duration GRBs. However, the association of rare type Ic supernovae with several long GRBs (e.g., Hjorth et al. 2003) suggests that these GRBs indicate the formation of compact objects following stellar collapse. This hypothesis, based on the Collapsar model (Woosley 1993), suggests that the progenitor of long duration GRBs are Wolf–Rayet stars (e.g., Chevalier & Li 1999). In addition, other astrophysical phenomena can mimic GRBs, such as the magnetic reconnection onto a neutron star (Usov 1992) or the tidal disruption of a minor body by a compact object (Boër et al. 1989). These events must occur at closer proximities than classical long GRBs as their available energy is lower.

We here present an analysis of the longest burst ever observed, GRB 111209A , which had a duration of 25000 s. This burst occurred at a redshift of $z = 0.677$ (Vreeswijk et al. 2011). Our analysis uses the observations of *XMM-Newton* (Jansen et al. 2001) and *Swift* (Gehrels et al. 2004) in the X-ray, Konus-*Wind* (Aptekar et al. 1995) in the gamma-ray band, and TAROT (Klotz et al. 2009) in the optical, as well as archived and public data. In this paper we focus our attention on the prompt emission of GRB 111209A to determine the most likely astrophysical source of such an ultra-long event. An additional paper will discuss the afterglow properties in a multiwavelength context (G. Stratta et al., in preparation).

In the following, we define the classes of bursts with durations greater than 2 s, 10^3 s, and 10^4 s as long, super-long and ultra-long GRBs respectively. We also define T_{90} the time required to radiate 90% of the total energy observed in a given band. We assume flat Λ CDM universe with $H_0 = 71$ km s^{-1} Mpc^{-1}, $\Omega_m = 0.27$, and quote all errors at the 90% confidence level. The outline of the paper is as follows.

In Sections 2 and 3 we present the observations and the data reduction respectively. The data analysis is described in Section 4. We discuss the duration and scarcity of events like GRB 111209A in Section 5, and in Section 6 consider plausible scenarios for the progenitor of GRB 111209A. We present our conclusions in the final Section 7.

2. GRB 111209A

GRB 111209A was discovered by the *Swift* satellite at $T_0 =$ 2011:12:09–07:12:08 UT (Hoversten et al. 2011). This event initiated two triggers of the Burst Alert Telescope (BAT; triggers number 509336 and 509337). It showed an exceptionally long duration, was monitored up to $T_0 + 1400$ s. However, the burst started about 5400 s before T_0, as shown in the ground data analysis of the Konus-*Wind* instrument, and a reanalysis of the BAT data showed that GRB 111209A was detectable 150 s

[11] On personal leave; present address: rue de l eglise F-31480 Lagraulet St Nicolas, France.

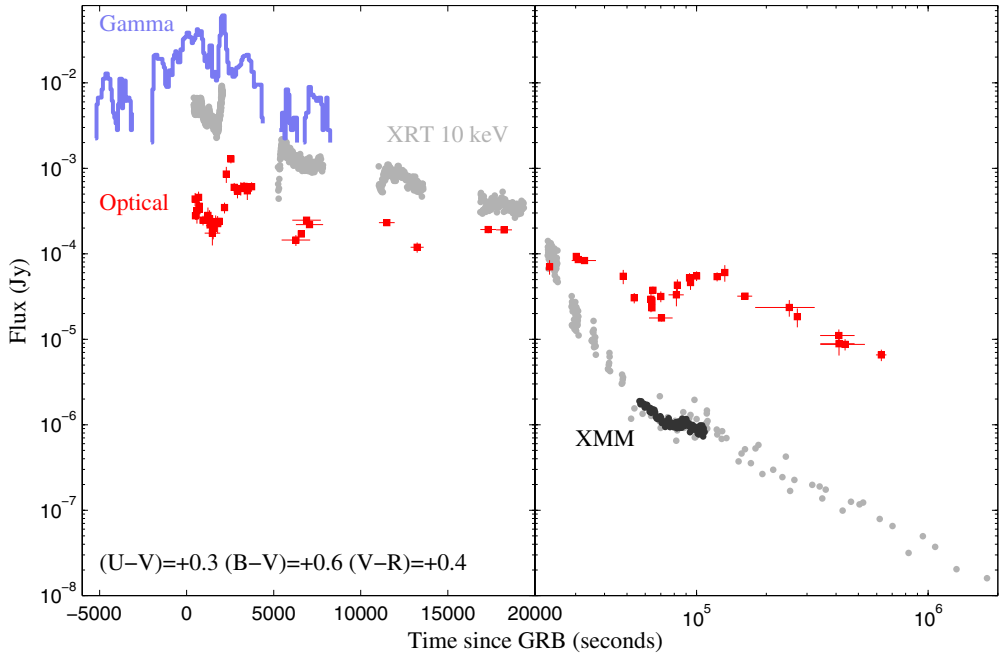

Figure 1. Light curve of GRB 111209A, presented with a temporal axis which is linear in the left panel (the prompt emission) and logarithmic in the right panel (the afterglow emission). X-ray data are in gray (XRT) and black (*XMM-Newton*). The Konus-*Wind* data (blue solid line) has been scaled to the X-ray data for comparison. The *R*-band light curve is constructed from TAROT and *Swift*/UVOT data (color indices are indicated on the plot).

(A color version of this figure is available in the online journal.)

before the trigger. *Swift* did not trigger at the start of the event as the burst was not in the field of view of the BAT instrument.

GRB 111209A was also detected by Konus-*Wind*. In order to compare the light curve of this event with other bursts, we used the publicly available soft band (21–83 keV; similar to the *Swift*/BAT 15–150 keV band) light curve. The earliest portion of the gamma-ray signal detected by Konus-*Wind* featured a weak broad pulse. The gamma-ray signal was then observed as a multi-peaked emission up to about T_0 + 10000 s (Golenetskii et al. 2011). Using the Konus-*Wind* results, GRB 111209A had a fluence of $(4.86 \pm 0.61) \times 10^{-4}$ erg cm^{-2}, an isotropic energy $E_{\rm iso} = (5.82 \pm 0.73) \times 10^{53}$ erg, and an intrinsic peak of the spectrum in the νf_ν space of $E_p = 520 \pm 89$ keV (Golenetskii et al. 2011). These values are in agreement to within 2σ with the Amati relation (Amati et al. 2002) which empirically links these last two quantities for long GRBs.

Swift/XRT observations started 425 s after the BAT trigger (Hoversten et al. 2011) revealing a bright afterglow, observed also by *Swift*/UVOT in the optical–UV bands at R.A. (J2000) = $00^{\rm h}57^{\rm m}22\overset{\rm s}{.}63$ and Decl. (J2000) = $-46^{\rm d}48'03\overset{''}{.}8$, with an estimated uncertainty of $0\overset{''}{.}5$. The afterglow was also clearly detected by ground based instruments; for example, the TAROT-La Silla (Klotz et al. 2011), and the GROND robotic telescopes (Kann et al. 2011). In addition, we activated a Target of Opportunity observation with *XMM-Newton*, between T_0 + 56, 664 s and T_0 + 108, 160 s (see the light curve in Figure 1). This period covered the end of the prompt phase seen in X-ray, a subsequent plateau phase, and the start of the normal afterglow decay (Gendre et al. 2011).

3. DATA REDUCTION

3.1. Swift/XRT

Swift/XRT data were taken as Level 1 event files from the Swift Data Center archive at NASA/GSFC and were processed with the task *xrtpipeline* version 0.12.6, applying the most updated calibrations. Data acquisition started in Windowed Timing (WT) mode and continued in this mode up to the fourth orbit (T_0 + 22700 s). XRT then switched to the Photon Counting (PC) mode for the remaining of the observation (up to 26 days after the trigger). Pile-up can be observed in WT mode during the first orbit (i.e., up to T_0 + 2000 s), and in PC between T_0 + 22700 s and T_0 + 30900 s. As a consequence, spectra and light curves were extracted using the methods of Romano et al. (2006) and Vaughan et al. (2006), excluding a central circle of radius 1 pixels from the point-spread function (PSF) in WT mode; for the PC mode, the radius was set dynamically between 7 and 1 pixels as a function of the flux of the afterglow, and the results were checked with the PSF profile of the XRT.

All spectra and light curves were then extracted using standard filtering and screening criteria (including bad columns and bad pixels), and corrected for telescope vignetting and aperture filtering using the ancillary response files (ARFs) generated by the task *xrtmkarf*. We then rebinned all files to either match the spectral resolution when the data quality was high enough, or to obtain at least 30 counts per bin.

3.2. XMM-Newton

We retrieved the Observation Data Files from the *XMM-Newton* archive and reprocessed them using the XMM-SAS version 12.0.1 and the latest available calibration files associated with this version of the SAS. The raw events files were processed using the tasks *emchain, epchain, rgsproc, omichain, omfchain*. The PN instrument observed GRB 111209A in Full Window mode, while the MOS cameras setting was on Small Window. Because of the brightness of the afterglow, we checked for pile-up in the data. We used the task *epatplot* for this purpose, and confirmed that the data were free from pile-up, even if a significant fraction of *out off time events* were observed. Because of this latter effect, the background regions have been chosen,

Table 1
X-Ray Spectral Analysis of GRB 111209A

Instrument Observing Mode	Start Time (s)	End Time (s)	Spectral Model	Γ	E_0 (keV)	Second Spectral Component (eV or energy index)	χ^2_ν (dof)
Swift/WT	425	1000	BKN+BB	1.17 ± 0.03 1.52 ± 0.06	3.4 ± 0.4	30 ± 5	0.98 (181)
Swift/WT	5025	7825	PL	1.58 ± 0.03			1.13 (590)
Swift/PC	22700	25130	PL	1.8 ± 0.1			0.87 (50)
Swift/PC	28780	30880	PL	1.9 ± 0.1			0.78 (32)
XMM-Newton	55073	61416	2PL	0.9 ± 0.7		2.7 ± 0.2	0.89 (151)
XMM-Newton	61416	66416	2PL	$1.2^{+0.7}_{-0.9}$		$2.8^{+0.4}_{-0.2}$	0.84 (111)
XMM-Newton	66416	71416	2PL	$1.9^{+0.4}_{-0.8}$		$3.3^{+0.9}_{-0.5}$	0.86 (95)
XMM-Newton	71416	76416	2PL	$1.7^{+0.5}_{-0.9}$		$3.1^{+0.8}_{-0.4}$	1.05 (83)
XMM-Newton	76416	91416	2PL	$1.7^{+0.5}_{-0.7}$		$3.0^{+0.5}_{-0.3}$	0.89 (228)
XMM-Newton	91416	108599	2PL	$2.3^{+0.3}_{-0.8}$		$3.4^{+1.3}_{-0.6}$	1.04 (234)

when possible, far away from the source and corrected for the difference of off-axis angle using the ARFs. In the special case of the PN instrument, the instrumental background is highly variable depending on the position on the instrument—this was taken into account by using a region where the instrumental background was compatible with the position of the source.

We then checked for flares of solar protons which can induce a huge increase of the background count rate, and found some marginal events where the background rate was increased by a factor of five. Due to the brightness of the afterglow, these events are not very significant for the following analysis: when maximal, the background represents around 6% of the total signal at the position of the afterglow.

The event files were then filtered for good photons, using FLAG == 0 and Pattern filtering (less than 4 for the PN, less than 12 for the MOS). Spectra were extracted using the task *especget*, light curves with the task *evselect*.

4. DATA ANALYSIS

4.1. Temporal Analysis

GRB 111209A X-ray emission indicates an initial shallow decay phase. Assuming a power-law model between T_0 + 0.425 ks and T_0 + 10.4 ks, the best-fit decay index is $\alpha_p = 0.544 \pm 0.003$. This phase ends very late in comparison with typical X-ray emissions. At the end of this phase, a gradual steepening drives the light curve to the so called "steep decay" phase, thought to indicate the end of the prompt emission and is characterized by very fast decrease of the count rate. During this phase and the following one, the light curve can be modeled with a double broken power law with a steep decay index of $\alpha_s = 4.9 \pm 0.2$, a plateau with decay index of $\alpha_f = 0.5 \pm 0.2$, and a final decay index of $\alpha_a = 1.51 \pm 0.08$.

4.2. Spectral Analysis

In the following, all models fitted to the data were multiplied by two components in order to take into account our Galaxy and the host galaxy photoelectric absorption from metals. The equivalent hydrogen column density of our Galaxy was set to $N_{\rm H} = 1.48 \times 10^{20}$ cm^{-2} (Kalberla et al. 2005). The second absorption component was left free to vary at the redshift of the burst, assuming solar metallicity. We found no temporal variation of the intrinsic $N_{\rm H}$, with a mean of $(2.5 \pm 0.4) \times 10^{21}$ cm^{-2}.

We began with an analysis of the prompt spectral emission between T_0 and T_0 + 2500 s, seen by *Swift*/XRT. GRB 111209A shows a strong flare at T_0 + 1200 s. Since flares are known to have highly variable spectra, this was excluded in order to investigate the underlying spectral continuum. The spectrum was of exceptionally high quality, and was rebinned in order to obtain at least 400 counts per bin. The background subtracted energy spectrum between T_0 + 425 s and T_0 + 1000 s is inconsistent with a simple power-law or cutoff power-law model. The best-fitting model was that based on a broken power law added to a blackbody component. The high-energy segment of the broken power law is consistent with the BAT spectrum at the same time ($\Gamma = 1.48 \pm 0.03$; Palmer et al. 2011), but harder than the time-averaged Konus-*Wind* best-fit model. We note however that the following spectra (extracted between 5.0 and 47.8 ks) are softer, consistent with the time averaged Konus-*Wind* spectrum. We therefore assume that the spectral position of the break (i.e., $E_{\rm break}$) varies with time, and that this break is due to the crossing of a specific frequency within the observed band. The blackbody component is very soft (see Table 1 and Figure 2), and accounts for about 0.01% of the total flux in the 0.5–10.0 keV band. Its luminosity is $\sim 1.6 \times 10^{50}$ erg s^{-1}. Moreover, this component is not detected at later times.

The *XMM-Newton* monitoring period covered the transition from the steep decay phase to the "normal" decay phase, for an interval of 53,000 s. Because of the greater sensitivity of *XMM-Newton* in comparison with the *Swift*/XRT, we were able to extract the spectra in six different time intervals (see Table 1). A simple power-law model was first used, giving an acceptable value of the χ^2 statistic value. However, the residuals of the fit clearly showed systematic excesses at the hard end of the spectrum, and thus a double component model was preferred. The inclusion of a second component produced an F-test probability (the probability that the decrease of the χ^2 statistic value is due to a spurious effect) of the order of 10^{-9}. The spectral fit clearly indicates that this second component is not dominating, and provides a small contribution to the total observed flux.

We extracted a spectral energy distribution (SED) during the *XMM-Newton* observation using published results from Kann et al. (2011) in the optical, in order to confirm no thermal emission was present during this phase. Kann et al. (2011) already noted that the GROND data excluded a thermal component, and indeed we have found an optical spectral index of $\beta = 1.1 \pm 0.2$, using the optical data alone. Using the X-ray

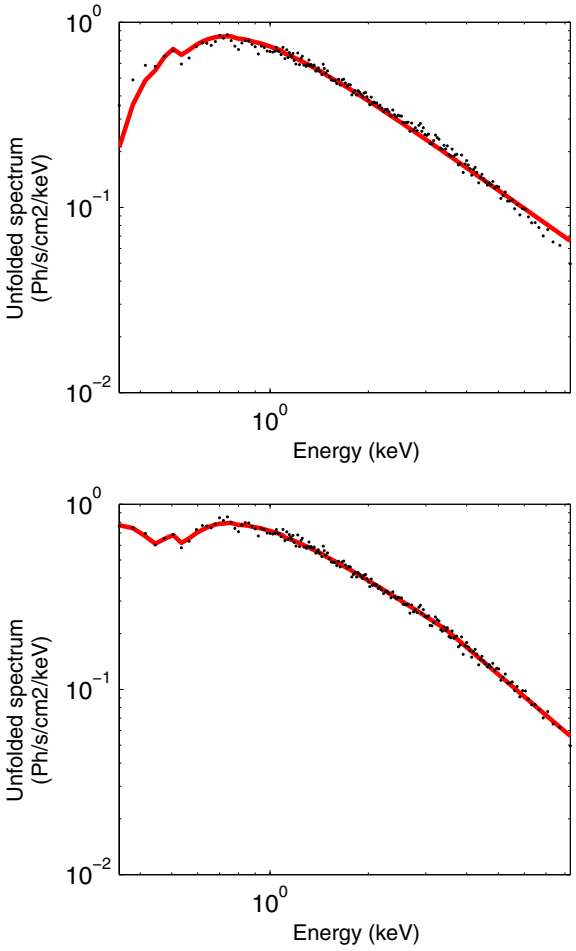

Figure 2. *Swift*/XRT WT spectrum. The spectrum is fitted with a simple power law (upper panel) or with the addition of a blackbody and a broken power law (lower panel). An improvement fit is clearly visible in the bottom panel.

(A color version of this figure is available in the online journal.)

to optical data, we found that an absorbed broken power law fitted the data well. We note that we can exclude the presence of a thermal emission in the far UV or the soft X-ray parts of the broad band spectrum.

As stated previously, this paper focuses on the properties of the progenitor of GRB 111209A, and the nature of this second component will be investigated in more detail in a forthcoming paper (G. Stratta et al., in preparation). We note however that this is the first time, to date, that such a double non-thermal component has been detected during the steep decay phase. Several models can account for it (e.g., see the model of Barniol Duran & Kumar 2009). The optical light curve features a rebrightening during the *XMM-Newton* observation: this component may be linked to the prompt-to-afterglow transition, to the optical bump, or even be totally unrelated to these components.

5. DISCUSSION

5.1. Duration of the Prompt Emission

The estimation of the burst duration using classical methods (i.e., T90) is complicated by two factors: it is well known that the duration depends on the observing band (the softer the band, the longer the detected signal); and for this event the prompt phase is split into several orbits, with gaps in the signal. Significantly, the event was recorded by Konus-*Wind* before T_0, when the burst was not in the field of view of *Swift*/BAT. Therefore, all attempts to use classical methods are flawed. To give an estimate of the total duration for comparison with other bursts, we thus estimated the burst start and stop epochs $T_{\rm start}$ and $T_{\rm end}$ as follows:

1. For $T_{\rm start}$, we use the start of the detection by Konus-*Wind*, about 5400 s before T_0.
2. For $T_{\rm end}$, we use the time of the start of the sharp decay, about 20,000 s after T_0.

The choice of the $T_{\rm end}$ value is motivated by the fact that the sharp decline is usually interpreted as the high-latitude emission of the prompt phase, and its start time corresponds to the true end of the prompt phase (Kumar & Panaitescu 2000). Before the steep decay phase, the initial XRT and BAT light curves are usually well correlated, indicating a common origin. This is also the case for GRB 111209A (see Figure 1). With these assumptions, the total duration of GRB 111209A is at least 25,000 s.

We extensively surveyed the *Swift*, BATSE, and Konus-*Wind* catalogs to find other ultra-long bursts. The most complete and homogeneous catalog of prompt burst properties is the BATSE 4B catalog (Paciesas et al. 1999). From this catalog, only few bursts have a duration larger than 1000 s (the super-long ones), and none have a duration longer than 10,000 s. For the case of *Swift*, we also searched in the XRT light curve repository (Evans et al. 2007) to obtain the start time of the sharp decay for all bursts, and found no burst with such a large duration. Thus, GRB 111209A is to date the longest confirmed GRB ever observed, and its duration is exceptional.

We note, however, for completeness, that one event, longer than GRB 111209A, has a debated origin. Swift J164449.3+573451 (hereafter J1644+57) has been proposed by several groups to be a tidal disruption event (e.g., Burrows et al. 2011; Bloom et al. 2011; Levan et al. 2011; Tchekhovskoy et al. 2013). Nevertheless Quataert & Kasen (2012), even though agreeing that the most plausible origin was a tidal disruption event, have shown theoretically that the explosion of a massive star could produce a similar event.

5.2. Selection Effects on Ultra-long GRBs

It is possible that selection effects make only the brightest part of ultra-long burst light curves detectable, thus reducing their intrinsic durations and making ultra-long GRBs indistinguishable from normal bursts. We investigated this selection effect in two ways.

First, we constrained the maximum distance from which this burst could be detected. We extracted data from the Konus-*Wind* light curve, rescaling it to a given distance and then added the background of the instrument (adding statistical fluctuations in the final signal to take into account Poisson statistics). We used two signal levels: the original one, and a second level an order of magnitude fainter. The light curve was examined for a burst with a rate trigger threshold of 5σ. We used two different bin sizes for the light curve (1 and 2 minutes), the latter simulating more complex trigger methods where an image trigger can be considered. The simulation was performed 100 times for all redshifts between 0.3 and 2.2 (with a step of 0.1). Results are presented in Figure 3, and are quite clear: GRB 111209A cannot be detected at high-z. In fact, this event can be detected only within a limiting redshift of $z = 1.4$.

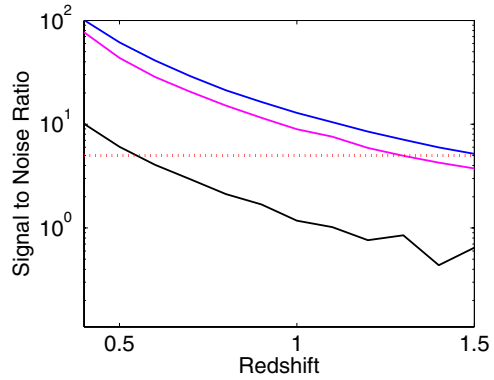

Figure 3. Detection significance expressed in signal to noise ratio units for a GRB 111209A like event as a function of its redshift. We present the detection regime of such bursts using light curve bin sizes of 1 minute (purple line) and 2 minutes (blue line); and a burst 10 times fainter with 2 minute bin size (black line). The dotted red line indicates our detection threshold (5σ level), showing that even in the optimal case the maximum redshift for detection is $z = 1.4$–1.5.

(A color version of this figure is available in the online journal.)

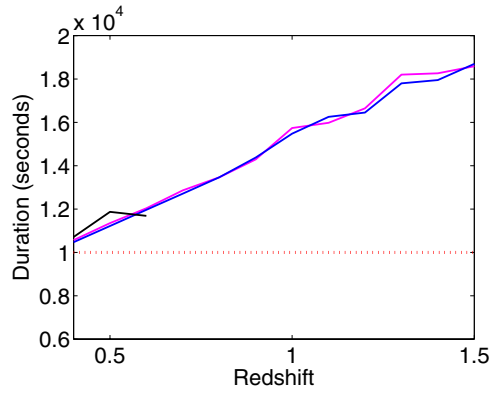

Figure 4. Measured duration of a GRB 111209A like event as a function of its redshift. Colors are the same as those in Figure 3. The horizontal red dotted line represent 10,000 s. The black line is truncated at the point where the errors are larger than the measured duration.

(A color version of this figure is available in the online journal.)

Second, for positive detections (at $z < 1.4$), we computed the expected duration of the burst, using the standard GRB procedure to obtain T90. Again, this is done for two distinct temporal resolutions and flux thresholds. Results are presented in Figure 4. Surprisingly, we find that the duration is larger than 10000 s in all cases. Thus, an ultra-long burst that could trigger an instrument would always be detected as an ultra-long GRB. The lack of such other bursts in ∼30 yr of archives indicates a very rare event in the local universe. Such events may have been more common in the distant universe, but their faintness makes their detection unfeasible.

5.3. The Rate of Ultra-long GRB in the Local Universe

We estimated the rate of ultra-long GRBs in the local universe using the properties of GRB 111209A. Taking into account the effect of the redshift on *Swift*'s sensitivity and *k*-correction (Coward et al. 2012; Howell & Coward 2013), this rate density can be inferred from the measured peak flux. We used the brightest epoch of the GRB 111209A prompt phase, as seen by Konus-*Wind*, scaled to the *Swift* energy band. This is then scaled to the limiting detection flux of *Swift* to obtain a maximal redshift for detection for *Swift*, $z_{\rm lim}$ (see Coward et al. 2012, for details). The corresponding volume of detectability is then:

$$V_{\rm max} = \int_0^{z_{\rm lim}} \frac{dV}{dz} dz. \quad (1)$$

Using the cosmological model provided in the Introduction, the maximum detectable volume corresponding to $z_{\rm lim} = 1.4$ is $V_{\rm max} = 292$ Gpc^3. Following Guetta & Della Valle (2007); Coward et al. (2012) we calculate a rate density

$$R = \frac{1}{V_{\rm max}} \frac{1}{T} \frac{1}{\Omega} \frac{1}{\eta_z}, \quad (2)$$

with T the maximum observation-time for the sample (7 yr), $\Omega = 0.17$ the sky coverage of the instrument and $\eta_z = 0.3$ the fraction of *Swift* bursts with a measured redshift. We obtain $9^{+27}_{-8} \times 10^{-3}$ Gpc^{-3} yr^{-1} where the errors are the 90% Poisson confidence limits (Gehrels 1986).

As only four out of 644 *Swift* bursts detected between the launch of the satellite and 2012 March have prompt emission durations greater than some thousands of seconds, we obtain the final rate for ultra-long GRBs to be of the order of $4 \times R/644 \sim 6 \times 10^{-5}$ Gpc^{-3} yr^{-1}. This is significantly lower than that of the normal long GRB rate density (see Howell & Coward 2013).

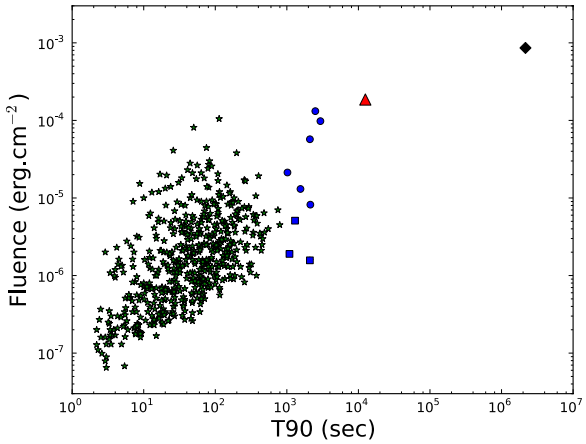

Figure 5. Position of GRB 111209A (red triangle) in the GRB fluence–duration plane. The green stars are long *Swift* bursts. Blue circles and squares are the recorded super-long GRBs, and the black dot is J1644+57. Blue squares represent high-energy transients attributed to supernova shock breakout. Note that all measurements are converted to the *Swift* band (15–150 keV) for comparison with the *Swift* catalog—therefore some values will differ from those given in Table 2.

(A color version of this figure is available in the online journal.)

5.4. Comparison with Super-long Bursts

We retrieved from the literature the prompt emission information available for the nine super-long bursts (with duration larger than 1000 s) listed in Table 2. The fact that GRB 111209A is harder and more fluent than other bursts is another indicator of its uniqueness. In Figure 5 we also present these bursts in the duration–fluence plane. GRB 111209A appears as an outlier in the duration distribution, but not in the fluence distribution, where other super-long GRBs can have a similar (even if slightly smaller) fluence. We note that supernova shock breakouts have a much smaller fluence, weakening a possible link between this kind of progenitor and GRB 111209A. Once corrected for distance (when possible—several bursts lacked a good follow-up

Table 2
Summary of the Prompt Properties of All Bursts with Duration Larger than 1000 s

Quantity	E_p (keV)	E_{iso} (10^{51} erg)	Fluence (erg cm^{-2})	Duration (T90, s)	Distance (redshift)	Reference
GRB 971208	144	n.a.	2.6×10^{-4}	2500	n.a.	Pal'Shin et al. (2008)
GRB 020410	n.a.	n.a.	2.8×10^{-5}	1550	n.a.	Nicastro et al. (2004)
GRB 060218	4.9	0.062	1.7×10^{-5}	2100	0.0331	Campana et al. (2006)
GRB 060814B	341	n.a.	2.4×10^{-4}	2944	n.a.	Pal'Shin et al. (2008)
GRB 080407	287	n.a.	4.5×10^{-4}	2100	n.a.	Pal'Shin et al. (2012)
GRB 090417B	>150	>7.3	8.2×10^{-6}	>2130	0.345	Holland et al. (2010)
GRB 091024	280	350	1.1×10^{-4}	1200	1.09	Golenetskii et al. (2009)
GRB 100316D	10–42	0.049	5.1×10^{-6}	1300	0.0591	Starling et al. (2011)
GRB 101225A	38	n.a.	2.6×10^{-6}	>2000	n.a.	Campana et al. (2011); Thöne et al. (2011)
Swift J1644+57	n.a.	n.a.	8.6×10^{-4}	2160000	0.354	Burrows et al. (2011)
GRB 111209A	520	580	4.9×10^{-4}	>25000	0.677	This work

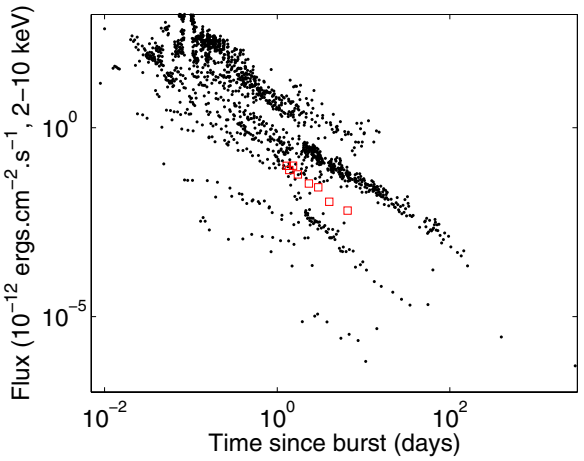

Figure 6. Absolute flux of GRB 111209A. Following the method of Gendre et al. (2008a), we rescale the X-ray afterglow light curve of GRB 111209A to a common distance of $z = 1$. This light curve is represented by red squares, while the sample of Gendre et al. (2008a) are shown as black dots.

(A color version of this figure is available in the online journal.)

campaign and thus a redshift measurement), this burst also appears to be more energetic than the others.

We also investigated the X-ray afterglow properties of these bursts. As shown in previous works using infrared, optical, and X-ray data, the luminosity of afterglows tends to cluster in several groups (Boër & Gendre 2000; Gendre & Boër 2005; Liang & Zhang 2006; Nardini et al. 2006; Gendre et al. 2008a, 2008b). If one includes the X-ray light curve of GRB 111209A in the sample of Gendre et al. (2008a; see Figure 6), the event is shown to be marginally under luminous. However, this could be interpreted as a normal consequence of the duration of the prompt phase. In this phase, internal shocks dissipate the energy of the fireball. The longer the prompt phase lasts, the less energy remains to be dissipated within the following external shock.

6. NATURE OF THIS EVENT

In the following section, we investigate the possible progenitors of such an ultra-long event.

6.1. Thermal Components

The first hypothesis is that the exceptional duration of GRB 111209A is due to a component usually not present in normal GRBs. Two super long GRBs (GRB 060218, $z = 0.033$, and GRB 100316D, $z = 0.059$) were associated with a supernova shock breakout (Campana et al. 2006; Starling et al. 2011). These two events are also classified as sub-energetic (Howell & Coward 2013), with very soft X-ray spectra, and their prompt spectra (including the steep decay) show a thermal emission, which is responsible for the long duration. We also do observe a thermal component at the start of the XRT observation; however this component disappears very soon, and most of the prompt phase is free of thermal emission. We can therefore discard this hypothesis.

Starling et al. (2012) have found in several GRBs associated with a supernova a thermal component. They explain it as a hot plasma cocoon associated with the jet. However, they observe this component in the steep decay phase (where we do not see any thermal emission from GRB 111209A using *XMM-Newton* data), which is harder and dimmer than the one we detect at the start of the prompt phase. Thus, this model cannot be applied to GRB 111209A.

GRB 101225A, another super-long burst (Racusin et al. 2010), shows a strong optical thermal component. The lack of a redshift measurement for this burst made difficult to draw any conclusions on the explosion mechanism and two very different models were proposed: a minor-body tidal disruption by a neutron star in our galaxy (Campana et al. 2011), and the merger of a neutron star with a helium star in a distant galaxy (Thöne et al. 2011).

Apart from the lack of any strong thermal emission at optical (and X-ray) wavelengths, GRB 111209A differs from GRB 101225A as it is at least 10^3 times more energetic (using the most distant scenario of Thöne et al. 2011), suggesting a different origin for GRB 111209A.

6.2. Magnetars

In recent years, evidence has emerged that magnetars could account for long GRB properties (e.g., Metzger 2010). This class of progenitor provides a natural explanation of extended emissions as long lasting energy injection (Dall'Osso et al. 2011; Metzger et al. 2011). Indeed, if the typical duration of a long GRB powered by a magnetar is of the order of 40–100 s, atypical values of the magnetic field and spin period could allow a duration of ~25,000 s. However, such atypical values cannot fit both the observed values of E_{iso} and E_p. For instance, using the formalism of Metzger et al. (2011), reproducing the observed values of E_{iso} and duration would lead to $E_p \sim 180$ keV, that is a factor of three lower than the rest frame peak energy of GRB 111209A (520 keV). Trying to conciliate these values results in nonphysical solutions (e.g., a neutron star spinning at

a value exceeding the breakup value, $P_{\rm lim} = 0.96$ ms, Lattimer & Prakash 2004).

Another possibility would be to consider the long duration of the prompt phase as a plateau phase (i.e., assume the true prompt phase has been missed by all instruments). However, the magnetar model indicates that once the plateau phase is finished the decay should be monotonic with a decay index of 1–2 (Dall'Osso et al. 2011). This is in contradiction with our findings from the light curve (decay of $\alpha = 4.9 \pm 0.2$ with the presence of a following plateau).

Troja et al. (2007) has proposed a solution (later extended by Lyons et al. 2010) to this problem, with a two-stage progenitor: the collapsar would produce a magnetar that would collapse into a black hole a few hundreds of seconds later. Under this scenario one could expect a double plateau, i.e., a non-monotonic decay after the first plateau phase. The first plateau, due to the energy injection by the magnetar, would then be the observed prompt signal. However, again, one needs atypical values of the magnetic field and spin period to explain the observed properties of this event, and again this would produce inconsistent values of $E_{\rm iso}$ and E_p, not observed in this event. Significantly, the "first plateau" has also been observed in the gamma-ray band (it is the prompt signal), which is itself unique, making GRB 111209A a very peculiar event.

We thus conclude that a magnetar progenitor for GRB 111209A is not supported by the data.

6.3. Tidal Disruption Event

Swift J1644+57 was at first claimed to be a GRB. It is thus possible that GRB 111209A is not a GRB but a tidal disruption event. This solution is, however, not very convincing. Firstly, no host galaxy has been detected, while one may expect a massive black hole to lie in a galaxy bright enough to be detected at small redshift. Second, the light curve should decay as $t^{-5/3}$ (Lodato et al. 2009). This is however not the case (see Section 4). In fact, Swift J1644+57 did not show the characteristic GRB light curve behavior (so called steep-flat-steep, Zhang 2007) clearly visible in the case of GRB 111209A. For these reasons we can discard this hypothesis.

6.4. Giant Stars

The main difficulty in explaining the nature of the progenitor of GRB 111209A is its duration. Woosley & Heger (2012) investigated scenarios to provide a long duration event with an energy budget typical of a long GRB. They proposed four scenarios:

1. single supergiant stars with less than 10% solar metallicity;
2. supergiant systems in tidally locked binaries;
3. pair instability in very high mass stars resulting in collapse to a black hole;
4. helium stars in tidally locked binaries.

Scenarios (2) and (4) lead, assuming a typical values of 1% $\dot{M}c^2$ for the energy conversion efficiency, to luminosities orders of magnitude too faint in comparison to the that observed in the case of GRB 111209A. Only a 100% energy conversion efficiency would marginally reconciliate these numbers. As for scenario (3), at a distance of $z = 0.677$, one would expect a bright optical supernova easily detectable with large aperture telescopes. Despite follow-up of GRB 111209A by the *Hubble Space Telescope* and the Very Large Telescope, no evidence of a supernova was claimed (Levan 2012). The above arguments leave us with scenario (1), a single supergiant star with low metallicity. We note that Quataert & Kasen (2012) used the same kind of progenitor to discuss the link between Swift J1644+57 and a GRB.

The hypothesized progenitors of long duration GRBs are Wolf–Rayet stars (stars with the outer layers expelled during stellar evolution). When these layers are still present, as in low-metallicity supergiant stars with weak stellar winds, the stellar envelope may fall back and accretion can fuel the central engine for a much longer time. In this scenario, blue supergiant stars can produce GRBs with prompt emission lasting about 10^4 s (Woosley & Heger 2012).

Theoretically, a larger star, such as a red supergiant star could also be considered, assuming that the outer layers are expelled in order to maintain the free-fall time scale to the order of 10^4 s. For instance, a very weak explosion could eject the convective envelope of a red supergiant without producing an observable supernova, (e.g., Dexter & Kasen 2012). However, in such a case, this layer of matter is still surrounding the progenitor of the GRB, making the surrounding medium density profile much more complex. As shown by e.g., Chevalier et al. (2004), these complex geometries should imprint their mark on the afterglow light curve, and in fact do (see for instance GRB 050904, Gendre et al. 2007). Here we do not see this complex afterglow behavior, supporting the suggestion of a simple blue supergiant star.

If one considers the ratio of normal GRBs to ultra-long GRBs, this is shown in the *Swift* archives to be of the order of 200:1. In comparison, the fraction of blue supergiants compared to Wolf–Rayet stars is typically 10:1 (Eldridge et al. 2008)—therefore ultra-long GRBs should be more frequent than normal long GRBs. At first consideration, these numbers are difficult to reconcile. However, the greatest uncertainty of supergiant collapsars is whether matter with high angular momentum will be ejected by mass loss or will fall into the center of the star (Woosley & Heger 2012). It is plausible that for most of blue supergiant stars there is no fall back of the external layers, and thus no long emission. Hence, the observed and the expected rates may be reconciled by assuming the external layers of most blue supergiants do not fall into the stellar core. A rare combination of exceptionally large rotation and small mass loss at the end of stellar evolution could lead to a GRB 111209A like event. These properties can be both achieved in case of a low-metallicity progenitor. This would also help reconcile the numbers, as most of the local universe blue supergiant stars are not observed with low metallicity. One should then consider if it is possible to have these low-metallicity stars in the local universe.

6.5. Low Metal Protogalaxies in the Local Universe

The most putative hypothesis on the above consideration is the presence in the local universe of a galaxy with a very low metallicity. In fact, blue supergiants have short lifetimes, and the only way of having a low-metallicity blue supergiant is to form it from low-metallicity gas. We must thus discuss the possibility of having very low metallicity galaxies in the local universe. If such galaxies should have been common in the early universe, the hierarchical galaxy formation model implies that these have merged to form the larger galaxies observed today (see, e.g., Klypin et al. 1999). However, as pointed out by several authors, such a mechanism is not efficient at 100% (e.g., Klypin et al. 1999; Diemand et al. 2007), and galaxies with a very low metallicity should still exist in the local universe. In fact, several of those are known (Morales-Luis et al. 2011), and one object (I Zw 18) has a measured oxygen abundance of 0.05 solar one (Izotov et al. 1997). These are local objects (with $z < 0.1$),

accounting for about 0.1% of all the local galaxies (Morales-Luis et al. 2011), thus reinforcing the idea that GRB 111209A is a very rare event.

Furthermore, as noted by Morales-Luis et al. (2011), the luminosity–metallicity relationship (Lequeux et al. 1979) implies that low-metallicity galaxies cannot be observed in the more distant universe. The fact that the host galaxy of GRB 111209A has not been resolved by the *Hubble Space Telescope* (Levan 2012) would then support this hypothesis: only the GRB afterglow was visible, and GRB 111209A traces the location of a putative (very) metal poor galaxy at large distance ($z = 0.677$). At this distance, this galaxy would not have been detected without the GRB which occurred in it.

7. CONCLUSION

We have presented multi-wavelength observations of GRB 111209A. From the prompt emission, we have shown that this event is the longest GRB ever detected. We have also demonstrated that such a burst would have been detected up to $z = 1.4$ as an ultra-long event. The lack of any ultra-long GRBs suggests that such events are very rare.

The spectrum shows a very soft thermal emission during the first thousands of seconds of the X-ray observations, not observed at later times. In addition, we have detected the presence of a puzzling second component seen in X-rays during the fast decay and the following plateau phase. This spectral signature is very uncommon and suggests an unusual nature for the progenitor of this burst.

Explaining these spectro-temporal properties is difficult in the standard collapsar model, and we propose that this event is representative of a new class of rare stellar explosion, that of a blue supergiant star with a very low metallicity. We stress that the presence of such a low-metallicity giant star at this distance of our Galaxy, although rare, is not impossible. Thus the progenitor of this event could represent the closest link ever discovered with rare population III stellar explosions (Suwa & Ioka 2011; Nakauchi et al. 2012). One should also note that this event would not have been detectable at large redshift with the current instrumentation available. Only new instruments with very large detection areas, such as *LOFT* (Feroci et al. 2012) would be capable of such observations. However, at redshift 12, GRB 111209A would have a duration of 10^5 s (i.e., more than one day) making such events very difficult to detect.

The data of GRB 111209A are very rich, and this paper has only investigated the most prominent part of it. In a second paper, we will present a detailed study of the afterglow and the broadband spectrum, thus deducing the properties of the emission mechanism and of the surrounding medium.

We thank the anonymous referee for valuable comments, and E. Troja for discussions. This work has been financially supported by ASI grant I/009/10/0 and by the PNHE. D.M.C. is supported by an Australian Research Council Future Fellowship. TAROT has been built with the support of the CNRS-INSU. We thank the technical support of the *XMM-Newton* staff, in particular N. Loiseau and N. Schartel.

Facilities: *Swift*, *XMM-Newton*, TAROT-Calern, TAROT-ESO

REFERENCES

Amati, L., Frontera, F., Tavani, M., et al. 2002, A&A, 390, 81
Aptekar', R. L., Frederiks, D. D., Golenetskii, S. V., et al. 1995, SSRv, 71, 265
Barniol Duran, R., & Kumar, P. 2009, MNRAS, 395, 955
Bloom, J. S., Giannios, D., Metzger, B. D., et al. 2011, Sci, 333, 203
Boër, M., & Gendre, B. 2000, A&A, 361, L21
Boër, M., Hameury, J. M., & Lasota, J. P. 1989, Natur, 337, 716
Burrows, D. N., Kennea, J. A., Ghisellini, G., et al. 2011, Natur, 476, 421
Campana, S., Lodato, G., D'Avanzo, P., et al. 2011, Natur, 480, 69
Campana, S., Mangano, V., Blustin, A. J., et al. 2006, Natur, 442, 1008
Chevalier, R. A., & Li, Z. Y. 1999, ApJ, 536, 195
Chevalier, R. A., Li, Z. Y., & Fransson, C. 2004, ApJ, 666, 369
Coward, D., Howell, E., Piran, T., et al. 2012, MNRAS, 425, 2668
Dall'Osso, S., Stratta, G., Guetta, G. D., et al. 2011, A&A, 526, 121
Dexter, J., & Kasen, D. 2012, ApJ, submitted (arXiv:1210.7240)
Diemand, J., Kuhlen, M., & Madau, P. 2007, ApJ, 657, 262
Eldridge, J. J., Izzard, R. G., & Tout, C. A. 2008, MNRAS, 384, 1109
Evans, P. A., Beardmore, A. P., Page, K. L., et al. 2007, A&A, 469, 379
Feroci, M., Den Herder, J. W., Bozzo, E., et al. 2012, Proc. SPIE, 8443, 85
Gehrels, N. 1986, ApJ, 303, 336
Gehrels, N., Chincarini, G., Giommi, P., et al. 2004, ApJ, 611, 1005
Gendre, B., Atteia, J. L., Boër, M., et al. 2011, GCN, 12638
Gendre, B., & Boër, M. 2005, A&A, 430, 465
Gendre, B., Galli, A., & Boër, M. 2008a, ApJ, 683, 620
Gendre, B., Galli, A., Corsi, A., et al. 2007, A&A, 462, 565
Gendre, B., Pelisson, S., Boër, M., Basa, S., & Mazure, A. 2008b, A&A, 492, L1
Golenetskii, S., Aptekar, R., Mazets, E., et al. 2009, GCN, 10083
Golenetskii, S., Aptekar, R., Mazets, E., et al. 2011, GCN, 12663
Guetta, D., & Della Valle, M. 2007, ApJL, 657, L73
Hjorth, J., Sollerman, J., Møller, P., et al. 2003, Natur, 423, 847
Holland, S. T., Sbarufatti, B., Shen, R., et al. 2010, ApJ, 717, 223
Hoversten, E. A., Evans, P. A., Guidorzi, C., et al. 2011, GCN, 12632
Howell, E. J., & Coward, D. M. 2013, MNRAS, 428, 167
Izotov, Y. I., Foltz, C. B., Green, R. F., Guseva, N. G., & Thuan, T. X. 1997, ApJL, 487, L37
Jansen, F., Lumb, D., Altieri, B., et al. 2001, A&A, 365, L1
Kalberla, P. M. W., Burton, W. B., Hartmann, D., et al. 2005, A&A, 440, 775
Kann, D. A., Klose, S., Kruehler, T., et al. 2011, GCN, 12647
Klebesadel, R., Strong, I., & Olson, R. 1973, ApJL, 182, L85
Klotz, A., Boër, M., Atteia, J. L., & Gendre, B. 2009, AJ, 137, 4100
Klotz, A., Gendre, B., Boër, M., & Atteia, J. L. 2011, GCN, 12637
Klypin, A., Kravtsov, A. V., Valenzuela, O., & Prada, F. 1999, ApJ, 522, 82
Kouveliotou, C., Meegan, C. A., Fishman, G. J., et al. 1993, ApJL, 413, L101
Kumar, P., & Panaitescu, A. 2000, ApJL, 541, L51
Lattimer, J. M., & Prakash, M. 2004, Sci, 304, 536
Lequeux, J., Peimbert, M., Rayo, J. F., Serrano, A., & Torres-Peimbert, S. 1979, A&A, 80, 155
Levan, A. 2012, in Proc. of the Liverpool GRB conference, www.astro.ljmu.ac.uk/grb2012/presentations/presentations/levan_liverpool2012.pptx
Levan, A. J., Tanvir, N. R., Cenko, S. B., et al. 2011, Sci, 333, 199
Liang, E., & Zhang, B. 2006, ApJL, 638, L67
Lodato, G., King, A. R., & Pringle, J. E. 2009, MNRAS, 392, 332
Lyons, N., O'Brien, P. T., Zhang, B., et al. 2010, MNRAS, 402, 705
Meszaros, P. 2006, RPPh, 69, 2259
Metzger, B. D. 2010, in ASP Conf. Ser. 432, New Horizons in Astronomy, ed. L. M. Stanford, J. D. Green, L. Hai, & Y. Mao (San Francisco, CA: ASP), 81
Metzger, B. D., Giannios, D., Thompson, T. A., Bucciantini, N., & Quataert, E. 2011, MNRAS, 413, 2031
Morales-Luis, A. B., Sanchez Almeida, J., Aguerri, J. A. L., & Munoz-Tunon, C. 2011, ApJ, 743, 77
Nakauchi, D., Suwa, Y., Sakamoto, T., Kashiyama, K., & Nakamura, T. 2012, ApJ, 759, 128
Nardini, M., Ghisellini, G., Ghirlanda, G., et al. 2006, A&A, 451, 821
Nicastro, L., in't Zand, J. J. M., Amati, L., et al. 2004, A&A, 427, 445
Paciesas, W. S., Meegan, C. A., Pendleton, G. N., et al. 1999, ApJS, 122, 465
Palmer, D. M., Barthelmy, S. D., Baumgartner, W. H., et al. 2011, GCN, 12640
Pal'Shin, V., Aptekar, R., Frederiks, D., et al. 2008, in AIP Conf. Proc. 1000, Gamma-Ray Bursts 2007 (Melville, NY: AIP), 117
Pal'Shin, V., Hurley, K., Goldstein, J., et al. 2012, in Proc. Gamma-Ray Bursts Conf. 2012, ed. M. Galassi, D. Palmer, & E. Fenimore, PoS(GRB 2012)040, http://pos.sissa.it/archive/conferences/152/040/GRB2012_040.pdf
Quataert, E., & Kasen, D. 2012, MNRAS, 419, L1
Racusin, J. L., Beardmore, A. P., Campana, S., et al. 2010, GCN, 11493
Romano, P., Campana, S., Chincarini, G., et al. 2006, A&A, 456, 917

Starling, R. L. C., Page, K. L., Pe'er, A., Beardmore, A. P., & Osborne, J. P. 2012, MNRAS, 427, 2950
Starling, R. L. C., Wiersema, K., Levan, A. J., et al. 2011, MNRAS, 411, 2792
Suwa, Y., & Ioka, K. 2011, ApJ, 726, 107
Tchekhovskoy, A., Metzger, B. D., Giannos, D., & Kelley, L. 2013, MNRAS, submitted (arXiv:1301.1982)
Thöne, C. C., de Ugarte Postigo, A., Fryer, C. L., et al. 2011, Natur, 480, 72
Troja, E., Cusumano, G., O'Brien, P. T., et al. 2007, ApJ, 665, 599
Usov, V. V. 1992, ApJ, 389, 635
Vaughan, S., Goad, M. R., Beardmore, A. P., et al. 2006, ApJ, 638, 920
Vreeswijk, P., Fynbo, J., & Melandri, A. 2011, GCN, 12648
Woosley, S. E. 1993, ApJ, 405, 273
Woosley, S. E., & Heger, A. 2012, ApJ, 752, 32
Zhang, B. 2007, ChJAA, 7, 1